IJMS 2021 8(1) 101 - 112

International Journal of Multidisciplinary Studies (IJMS)
Volume 8, Issue 1, 2021

A study of the performance of organometal trihalide perovskite solar cell due to defects in bulk $CH_3NH_3PbI_3$ (MAPI) perovskite layer

Adihetty N.L[1], Attygalle M.L.C[2*], Narayan N.S[3], Jha P.K[3]

[1]Faculty of Graduate Studies, University of Sri Jayewardenepura, Gangodawila, Nugegoda, Sri Lanka
[2]Department of Physics, Faculty of Applied Sciences, University of Sri Jayewardenepura, Gangodawila, Nugegoda, Sri Lanka
[3]Department of Physics, Faculty of Science, The Maharaja Sayajirao University of Baroda, Gujarat, India

ABSTRACT

In this numerical simulation research, we have investigated device performances of p-i-n type organometal trihalide perovskite solar cell by introducing deep and shallow defects in the bulk halide perovskite layer. The organometal halide perovskite solar cell device structure has Glass/ITO/PEDOT:PSS/Bulk-MAPI/2D-MAPI/PCBM/Ag. The open-circuit voltage of the solar cell was decreased due to both shallow and deep defects of the bulk-MAPI layer which increase the recombination of electron-hole pairs in the solar cell. The dark saturation current, which causes to reduce the open-circuit voltage of the solar cell, was increased due to the deep defects in the bulk-MAPI layer. Therefore, the power conversion efficiency of the solar cell can be enhanced by minimizing the deep defects in the bulk-MAPI layer, which can increase the open-circuit voltage of the solar cell by suppressing the effect of dark saturation current. We have verified that Shockley-Read-Hall (SRH) recombination is the most predominant recombination mechanism when only the deep defects are presented in the bulk-MAPI layer. Also, this investigation has proved, that Radiative recombination has become the most predominant recombination mechanism when the shallow defects are presented in the bulk-MAPI layer by completely omitting the deep defects of the bulk-MAPI layer. Finally, our model verified that the dark saturation current of the solar cell controls the open-circuit voltage when the recombination is occurring in the solar cell. Iodine interstitial defects that mainly act as deep defects in the bulk-MAPI layer should be minimized to increase the overall solar cell performance and power conversion efficiency of the organometal trihalide perovskite solar cell device.

KEYWORDS: *Perovskite-Based Solar Cell, Recombination, Dark Saturation Current, Defects, Power-Conversion Efficiency*

Corresponding author: Attygalle M.L.C, Email: lattygalle@sci.sjp.ac.lk

1 INTRODUCTION

Organometal trihalide perovskites have shown good performance due to their special material properties, which are long carrier diffusion length, tuneable optical bandgap, weak exciton binding energy, and good light absorption. These material properties of the halide perovskite cause to show good performance in photovoltaics. The halide perovskites are becoming one of the promising solar cell materials because they have shown low material cost, low processing cost, and higher power conversion efficiencies. National Renewable Energy Laboratory (NREL) has represented that the power conversion efficiency of the single-junction Perovskite solar cell has achieved 25.2% (Best Research-Cell Efficiency Chart).

Organometal trihalide perovskites have general formula as ABX_3 (Mitzi, 2004). The most popular organometal halide perovskite is methylammonium lead iodide ($CH_3NH_3PbI_3$), which is also called 3D-MAPI or bulk-MAPI. This material shows a major issue, which is moisture instability (Krishna et al., 2019). To overcome this stability issue of 3D halide perovskites, 2D Ruddlesden-Popper halide perovskites can be combined with 3D halide perovskites. 2D halide perovskites have acquired the attention to solving the instability of 3D halide perovskites because 2D halide perovskites can block the penetrating moisture (Quan et al., 2016, Cao et al., 2015, Koh et al., 2018, Adihetty et al., 2020). The combination of 2D and 3D halide perovskite layers has acquired more attention because the moisture stability of the 3D halide perovskite layer has been increased by the 2D halide perovskite layer, which acts as a protective layer to the 3D halide perovskite layer. 3D/2D halide perovskite solar cells have become a good alternative, because of their low cost, good performance, and long-term stability (Li et al., 2018). 3D-MAPI and 2D sheets of $CH_3NH_3PbI_3$ have been used to model this p-i-n type solar cell using numerical simulation software, that is, Solar Cell Capacitance Simulator (SCAPS-1D) (Niemegeers et al., 2014). Density Functional Theory (DFT) calculations and experimental studies have proved that different types of point defects in 3D-MAPI can create shallow defects and deep defects (Brakkee and Williams, 2020), which cause to reduce the overall solar cell efficiency. According to Photoluminescence (PL) curves and other studies, 2D-MAPI has shown low point defects and interfacial defects (Heo et al., 2019). These two materials are combined to get the long-term performance of solar cell devices (Zhang et al., 2018).

Three recombination mechanisms of the 3D-MAPI have been investigated in this study, which are Shockley-Read-Hall (SRH), Radiative, and Auger recombination. SRH recombination occurs due to impurities or lattice defects in the semiconductor materials. These defects can create defect states that have energy states, which lie within the bandgap. These defect states, which can trap holes/electrons, help to recombine the charge carriers. Also, the 3D-MAPI

contains defects that cause to occur SRH recombination because defects of the 3D-MAPI layer can create defect states, which can act as SRH recombination centers. In the Radiative recombination, an electron that is coming from the conduction band combines with a hole that is in the valence band. The radiative recombination rate depends on the concentration of conduction band electrons and valence band holes. In Auger recombination, three charge carriers are involved to occur in the recombination process. In the first step of Auger recombination, an electron that is in the conduction band recombine with a hole that is in the valence band. The emitted energy of the first step is transferred to another electron that is in the conduction band. As a result, that electron is excited into a higher energy level in the conduction band. Then it releases the energy and comes to the conduction band edge. This process is called Auger recombination. The effects of the above recombination mechanisms are considered in this study.

To reach the theoretical efficiency limits of methylammonium lead iodide (3D-MAPI) solar cells, the open-circuit voltage (V_{OC}) of the solar cell must be increased because it is controlled by non-radiative recombination. Most of the experimental and computational studies of the 3D-MAPI have identified defect states within the bandgap (Brakkee and Williams, 2020). In this study, our main objectives were to analyze the performance of the p-i-n solar cell structure with different defects in the 3D-MAPI layer and also to find the most predominant recombination mechanism in the 3D-MAPI layer by using available recombination parameters and defect studies of the 3D-MAPI. Also, we would give an analytical overview of the most important defect, which must be reduced in the 3D-MAPI layer, and the most predominant recombination mechanisms of the 3D-MAPI layer with different defect conditions.

2 MATERIALS AND METHODS

2.1 Modeling Photovoltaic Device

In this numerical simulation study, we have numerically modeled the 3D/2D Organometal halide perovskite solar cell structure as a series of Glass/ITO/PEDOT:PSS/Bulk-MAPI/2D-MAPI/PCBM/Ag, which is shown in Figure 1. In this cell structure, PEDOT:PSS was used as a p-type organic hole transporting material (HTM), which is Poly (3,4-ethylenedioxythiophene) polystyrene sulfonate. The bulk (3D)-MAPI was employed as the main intrinsic absorber in which charge carriers are mainly generated. The 2D-MAPI layer has been utilized to reduce the degradation of the bulk (3D)-MAPI since 2D-MAPI can be used to block moisture. Also, the performance of the cell model can be altered by the 2D-MAPI layer thickness since 2D-MAPI can generate a portion of charge carriers by absorbing higher energy photons. PCBM has been operated as an n-type electron transporting material (ETM), which is a fullerene derivative (6,6)-phenyl-C61-butyric acid methyl ester. A Silver (Ag) electrode has been selected as back contact material by calculating the work function of the back contact (Niemegeers

et al., 2014). Indium-tin oxide (ITO) has been used as a transparent conducting oxide (TCO) (Girtan and Rusu, 2010, Chen et al., 2016). TCO was used as an optically transparent electrode that can allow admitting the photons and transport charge carriers through the solar cell. The solar cell model that contained optimized layer thicknesses was considered as the baseline solar cell model.

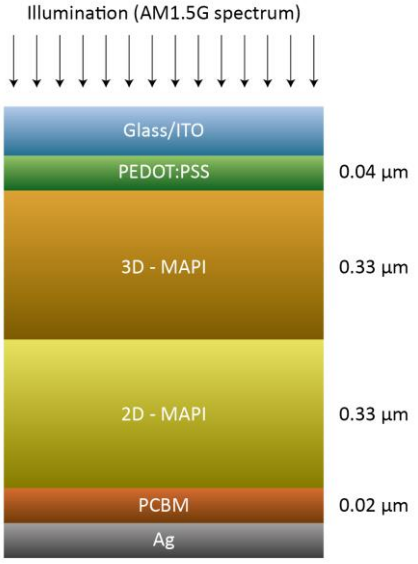

Figure 1: Device structure of the baseline solar cell model.

The Solar Cell Capacitance Simulator (SCAPS-1D) software has been used to model this solar cell. First, we have modeled the baseline cell model that was modeled without any defects in the semiconductor materials. Next, the same baseline model was simulated with only including shallow defects (single donor and single acceptor) into the 3D-MAPI layer. After that, the baseline model was simulated with only including deep defects, which are Amphoteric that is a type of multivalent defects, into the 3D-MAPI layer. In the next case, both shallow defects and deep defects (Amphoteric) were included in the 3D-MAPI layer. Here, we have studied how these two different types of defects in the 3D-MAPI layer affect to alter the open-circuit voltage (V_{OC}) and solar cell efficiency. The performance of 3D-MAPI was controlled by defects and carrier recombination. In this simulation study, we have included shallow defects and deep defects in the 3D-MAPI layer. But we have not considered any defects of the 2D-MAPI layer because the 2D-MAPI material has shown very low point defects and interfacial defects. Here we have studied how the cell performance was changed by different recombination mechanisms, which are occurring in the 3D-MAPI layer. We have investigated the effect of shallow and deep defects on the SRH recombination by considering different defect combinations in the 3D-MAPI layer. The effect of defects (deep, and shallow) on V_{OC} was studied by altering the defect type in the bulk-MAPI layer. The effects of other recombination mechanisms were also investigated by considering the combinations of different recombination mechanisms. Radiative-recombination coefficient (6×10^{-11} cm^3s^{-1}) and Auger-electron capture-coefficient (1.8×10^{-28} cm^6s^{-1}) of 3D-MAPI are extracted from previous research work (Tress, 2017).

2.2 Simulation

The SCAPS-1D simulation software was used to numerically simulate the solar cell model under the AM1.5G spectrum

condition. The SCAPS-1D software has been programmed by using mathematical relations as the Poisson equation, Continuity equation, and Transport equation (Niemegeers et al., 2014). The cell model was simulated by changing the defect type and recombination mechanism in the 3D-MAPI layer. The Shockley-Read-Hall (SRH), Auger, and Radiative recombination mechanism were considered, in the 3D-MAPI layer, to simulate the solar cell model.

3 RESULTS & DISCUSSION

3.1 Influence of Shallow Defects in the 3D-MAPI Layer

Here the effect of shallow defects in SRH recombination and the effect of other recombination mechanisms in 3D-MAPI was investigated. Donor and acceptor shallow defects of 3D-MAPI are located near to the conduction band and valence band, below 0.2 eV from the conduction band and above 0.1 eV from the valence band respectively. Shallow defects are created by some point defects, which are mainly vacancy defects (Kim et al., 2014). In this case, SRH recombination occurs via shallow defects because shallow defects are only included in the 3D-MAPI layer.

Table 1: Photovoltaic parameters of the solar cell model for different recombination mechanisms with the effect of the shallow defects in the 3D-MAPI layer.

		Photovoltaic parameters for different recombination mechanisms					
Added defects into 3D-MAPI	Without defect	Shallow defects	Without defects	Without defects	Shallow defects	Shallow defects	Shallow defects
Introduced recombination mechanisms into 3D-MAPI	Baseline model	SRH	Radiative	Auger	SRH+ Radiative	SRH + Auger	SRH + Radiative + Auger
V_{OC} (V)	1.2591	1.2584	1.1870	1.2318	1.1869	1.2315	1.1856
J_{SC} (mA/cm^2)	23.4881	23.5088	23.4881	23.4881	23.5088	23.5088	23.5088
FF (%)	83.55	83.47	84.94	85.11	84.88	85.01	84.96
Efficiency (%)	24.71	24.69	23.68	24.62	23.68	24.61	23.68

According to Table 1, shallow defects in the 3D-MAPI layer have caused to increase short circuit current (J_{SC}) of the solar cell model. However, the Fill factor (FF) of the cell model has been reduced by the shallow defects. Figure 2 illustrates that radiative recombination is the predominant recombination mechanism in this case because radiative recombination has reduced a considerable portion of cell efficiency. These results indicate that shallow defects do not affect to reduce a large portion of efficiency by SRH recombination. The efficiency reduction that happens due to SRH recombination is considerably lower than that of radiative recombination and Auger recombination. The effect of Auger recombination is more dominant than the SRH recombination. According to Figure 2, the V_{OC} has shown a considerable impact on solar cell efficiency when the recombination mechanisms are changed in the 3D-MAPI layer.

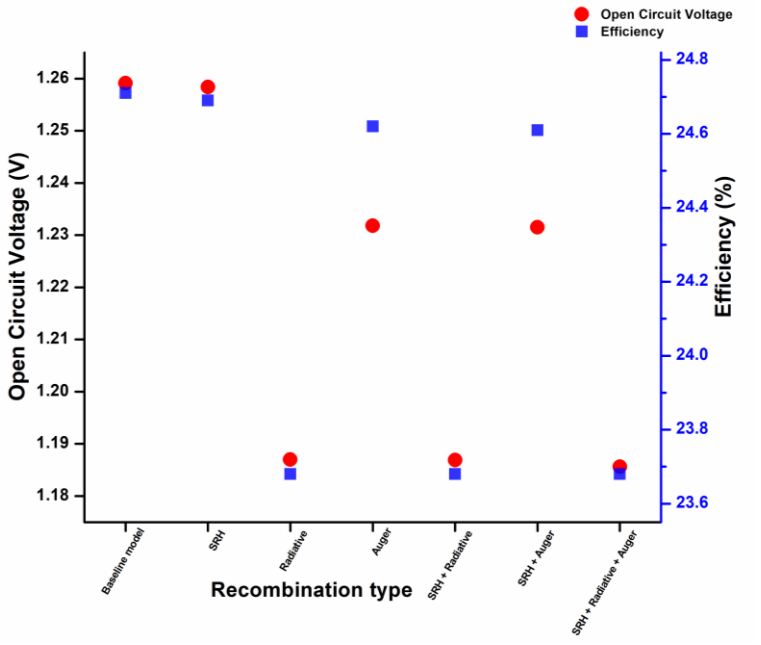

Figure 2: Open-circuit voltage (V_{OC}) and power conversion efficiency variation for different recombination mechanisms with the effect of shallow defects in the 3D-MAPI layer.

3.2 Influence of Deep Defects in the 3D-MAPI Layer

In this case, SRH recombination occurs only through the deep defect of the 3D-MAPI layer because deep defects are only included in the 3D-MAPI layer. According to the previous research work (Meggiolaro et al., 2018), Iodine interstitial defects ($I_i^+, I_i^0, and\ I_i^-$) have been identified as deep defects in 3D-MAPI, which have three different charge states (-1, 0, and +1). An amphoteric defect that is a type of multivalent-defects has been used to admit three different charge states of the defects, which cause to occur SRH recombination in the 3D-MAPI layer.

Table 2 shows that deep defects in the 3D-MAPI layer have caused to slightly increase short circuit current (J_{SC}) of the solar cell model. However, the Fill factor (FF) of the cell model has been considerably reduced by the deep defects. Figure 3 illustrates that SRH recombination has become predominant when deep defects are in the 3D-MAPI layer of the cell model because SRH recombination has reduced a large portion of V_{OC} and power conversion efficiency. The effect of radiative recombination is higher than the Auger recombination. These results indicate that deep defects should be minimized to increase cell efficiency. According to the diagram, the open-circuit voltage has become a critical factor when the recombinations are occurring in the 3D-MAPI layer.

Table 2: Photovoltaic parameters of the solar cell model for different recombination mechanisms with the effect of deep defects in the 3D-MAPI layer.

		Photovoltaic parameters for different recombination mechanisms					
Added defects into 3D-MAPI	Without defects	Deep defects	Without defects	Without defects	Deep defects	Deep defects	Deep defects
Introduced recombination mechanisms into 3D-MAPI	Baseline model	SRH only	Radiative only	Auger only	SRH + Radiative	SRH + Auger	SRH + Radiative + Auger
V_{OC} (V)	1.2591	1.0833	1.1870	1.2318	1.0825	1.0833	1.0825
J_{SC} (mA/cm^2)	23.4881	23.4915	23.4881	23.4881	23.4915	23.4915	23.4915
FF (%)	83.55	77.27	84.94	85.11	77.33	77.27	77.33
Efficiency (%)	24.71	19.66	23.68	24.62	19.66	19.66	19.66

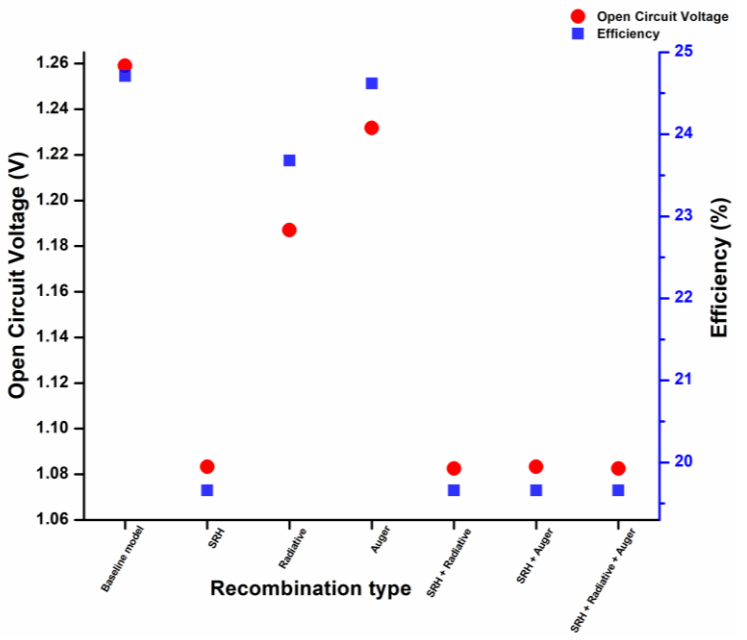

Figure 3: Open-circuit voltage (V_{OC}) and power conversion efficiency variation for different recombination mechanisms with the effect of deep defects in the 3D-MAPI layer.

3.3 Influence of Deep and Shallow Defects in the 3D-MAPI Layer

Here, the effect of both deep (Amphoteric) and shallow (single donor, and single acceptor) defects of 3D-MAPI have been investigated in SRH recombination because shallow and deep defects are included in the 3D-MAPI layer.

According to Table 3, that deep and shallow defects in the 3D-MAPI layer have considerably risen short circuit current (J_{SC}) of the solar cell model. The Fill factor (FF) of the cell model has been reduced by the deep and shallow defects in the 3D-MAPI layer. Figure 4 interprets that SRH recombination is the predominant recombination mechanism

when both deep defects and shallow defects are introduced into the 3D-MAPI layer. Deep defects highly affect SRH recombination than shallow defects. Here, the effect of SRH recombination is higher than the Auger or Radiative recombination.

Table 3: Photovoltaic parameters of the solar cell model for each recombination mechanism with the effect of the deep and shallow defects in the 3D-MAPI layer.

		Photovoltaic parameters for different recombination mechanisms					
Added defects into 3D-MAPI	Without defects	Deep and shallow defects	Without defects	Without defects	Deep and shallow defects	Deep and shallow defects	Deep and shallow defects
Introduced recombination mechanisms into 3D-MAPI	Baseline model	SRH only	Radiative only	Auger only	SRH + Radiative	SRH + Auger	SRH + Radiative + Auger
V_{OC} (V)	1.2591	1.0835	1.1870	1.2318	1.0835	1.0835	1.0826
J_{SC} (mA/cm^2)	23.4881	23.5121	23.4881	23.4881	23.5121	23.5121	23.5121
FF (%)	83.55	77.13	84.94	85.11	77.18	77.13	77.18
Efficiency (%)	24.71	19.65	23.68	24.62	19.65	19.65	19.65

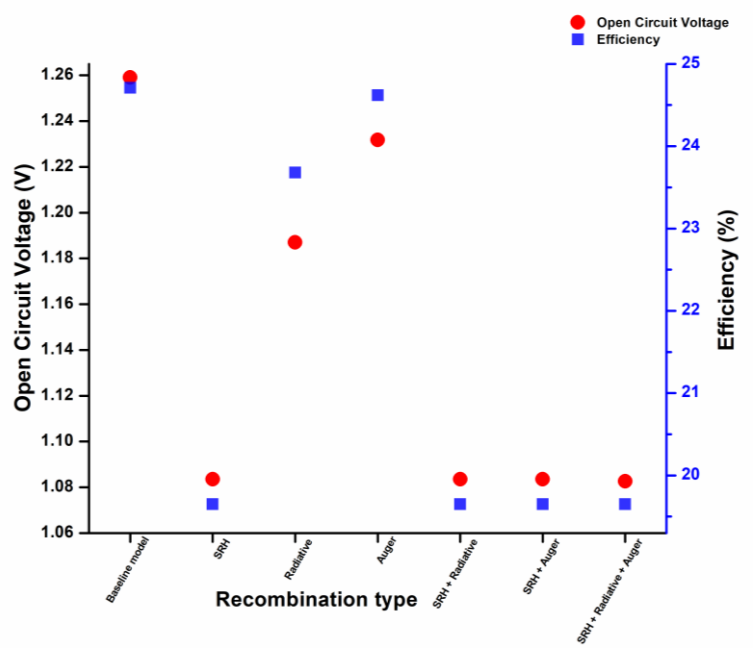

Figure 4: Open-circuit voltage (V_{OC}) and power conversion efficiency variation for different recombination mechanisms with the effect of shallow and deep defects in the 3D-MAPI layer.

3.4 Influence of Deep and Shallow Defects on Open-Circuit Voltage

Figure 2, Figure 3, and Figure 4 illustrate that the curves of efficiency vs recombination type have a similar shape to its open-circuit voltage (V_{OC}) vs recombination type curve.

$$V_{OC} = \frac{nkT}{q} \ln\left(\frac{J_L}{J_0} + 1\right)$$

Where n is the ideality factor, k is the Boltzmann constant, T is the temperature, and q is the electrical charge of the electron. According to the V_{OC} relation, the dark saturation current density (J_0) and light generated current density (J_L) are controlling the open-circuit voltage. Recombination in the solar cell can alter the dark saturation current density (J_0). The minimum V_{OC} can be expected when the solar cell shows the maximum dark saturation current.

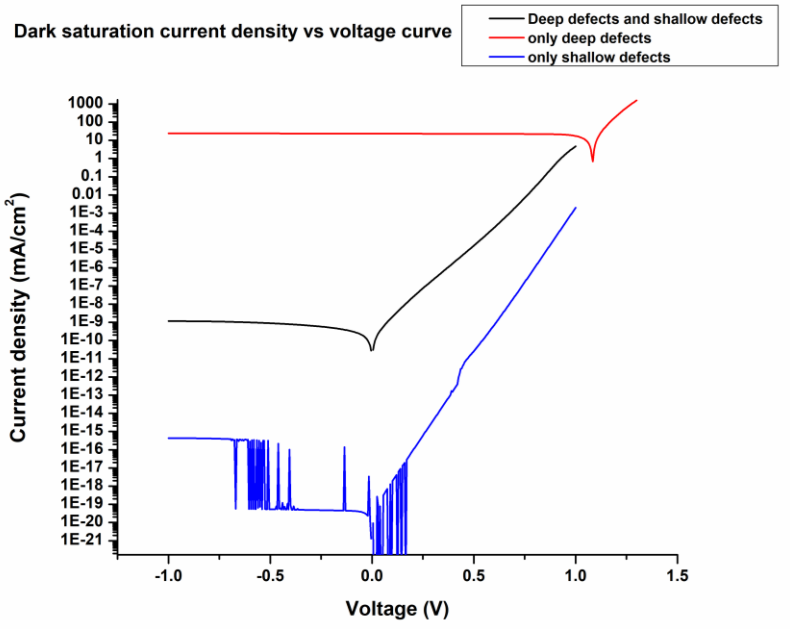

Figure 5: The semi-logarithmic current density vs voltage curve for dark saturation current density (J_O) with different defect conditions in the 3D-MAPI layer.

Figure 5, which was plotted by considering only SRH recombination with different defect combinations in the 3D-MAPI layer, illustrates that the dark saturation current vs voltage curves vary with the different defect combinations of the 3D-MAPI layer. According to the curve, maximum dark saturation current has been shown when the deep defects are in the 3D-MAPI layer, which indicates the minimum V_{OC} (1.0833 V) under the AM1.5G spectrum condition. Minimum dark saturation current has been shown when shallow defects are in the 3D-MAPI layer. Consequently, the maximum V_{OC} (1.2584 V) has been shown in this case. The dark saturation current was in between maximum dark saturation current and minimum dark saturation current when both deep and shallow defects were contained in the 3D-MAPI layer. The V_{OC} of both deep defects and shallow defects

curve (1.0835 V) is greater than that of the only deep defects curve. Also, the V_{OC} value can be used to measure the amount of recombination in a solar cell because a dark saturation current is used as a measure of recombination in a solar cell.

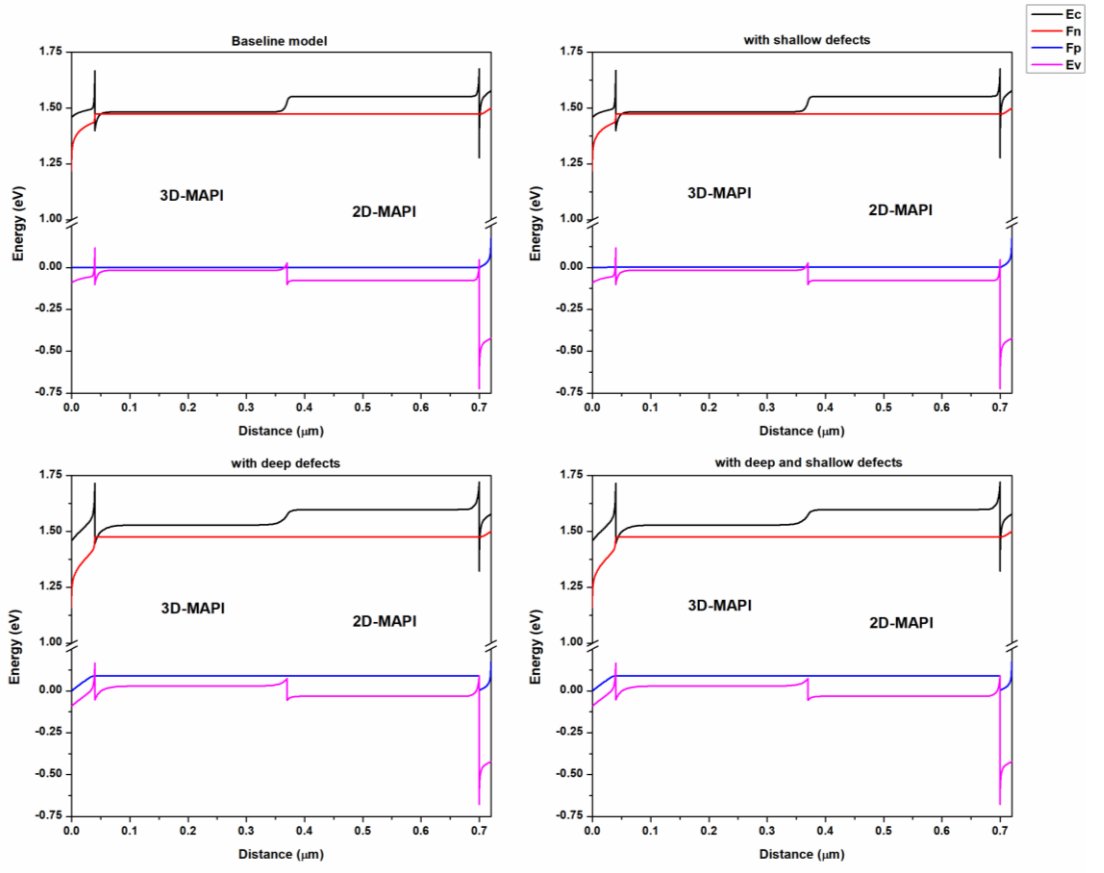

Figure 6: Energy band diagram of the cell model with different defects of 3D-MAPI (a) baseline model (without defects), (b) with shallow defects, (c) with deep defects, (d) with deep defects and shallow defects.

Figure 6 was plotted by considering only SRH recombination. Figure 6 (a) shows the energy bands of the baseline model. After adding shallow defects into 3D-MAPI, there is no considerable change in energy bands, in Figure 6 (b). But Figure 6 (c) indicates considerable changes of energy bands in the 3D-MAPI layer in which conduction band energy (E_C) and Quasi-Fermi level for holes (F_p) have been risen by deep defects, while valence band energy (E_V) and Quasi-Fermi level for electrons (F_n) have shown a slight change from Figure 6 (b). Similarly, Figure 6 (d) also shows approximately the same energy levels in the 3D-MAPI layer. Energy bands of the 3D-MAPI have been shifted upward in Figure 6 (c) and Figure 6 (d), which indicate that deep defects of 3D-MAPI can change the electric field in the 3D-MAPI layer. The change of the electric field limits the performance of the 3D-MAPI layer. And it should be

controlled to improve the overall cell efficiency.

4 CONCLUSIONS

In summary, deep defects can reduce a large amount of cell efficiency due to the Shockley-Read-Hall (SRH) recombination. According to the results, radiative recombination mainly causes to reduce cell efficiency when shallow defects are only introduced in the 3D-MAPI. And SRH recombination mainly affects to reduce power conversion efficiency of the cell model when deep defects are in the 3D-MAPI layer. Deep defects of materials should be minimized to get the better performance of the solar cell because they cause to increase dark saturation current in the solar cell. Also, the open-circuit voltage of the solar cell can be increased by reducing the deep defects.

REFERENCES

Adihetty, NL, Ratnasinghe, DR, Attygalle, MLC, Som, N & Jha, P 2020. Numerical Modeling of Thin Film Solar Cell with Hybrid 3D/2D Organic-Inorganic Halide Perovskite under Low Light Conditions and AM 1.5 G Full Sun Spectrum. *INTERDISCIPLINARY APPROACHES IN SCIENCE, ENGINEERING & HUMANITIES (ICIASEH-2020)*.

Best Research-Cell Efficiency Chart. *Photovoltaic Research* [Online]. Available: https://www.nrel.gov/pv/cell-efficiency.html [Accessed 24 December 2020.

Brakkee, R & Williams, RM 2020. Minimizing Defect States in Lead Halide Perovskite Solar Cell Materials. *Applied Sciences*, 10**,** 3061.

Cao, DH, Stoumpos, CC, Farha, OK, Hupp, JT & Kanatzidis, MG 2015. 2D homologous perovskites as light-absorbing materials for solar cell applications. *Journal of the American Chemical Society*, 137**,** 7843-7850.

Chen, A, Zhu, K, Shao, Q & Ji, Z 2016. Understanding the effects of TCO work function on the performance of organic solar cells by numerical simulation. *Semiconductor Science and Technology*, 31**,** 065025.

Girtan, M & Rusu, M 2010. Role of ITO and PEDOT: PSS in stability/degradation of polymer: fullerene bulk heterojunctions solar cells. *Solar Energy Materials and Solar Cells*, 94**,** 446-450.

Heo, S, Seo, G, Cho, KT, Lee, Y, Paek, S, Kim, S, Seol, M, Kim, SH, Yun, DJ & Kim, K 2019. Dimensionally Engineered Perovskite Heterostructure for Photovoltaic and Optoelectronic Applications. *Advanced Energy Materials*, 9**,** 1902470.

Kim, J, Lee, S-H, Lee, JH & Hong, K-H 2014. The role of intrinsic defects in methylammonium lead iodide perovskite. *The journal of physical chemistry letters*, 5**,** 1312-1317.

Koh, TM, Shanmugam, V, Guo, X, Lim, SS, Filonik, O, Herzig, EM, Müller-Buschbaum, P, Swamy, V, Chien, ST & Mhaisalkar, SG 2018. Enhancing moisture tolerance in efficient hybrid 3D/2D perovskite photovoltaics. *Journal of Materials Chemistry A,* 6**,** 2122-2128.

Krishna, A, Gottis, S, Nazeeruddin, MK & Sauvage, F 2019. Mixed dimensional 2D/3D hybrid perovskite absorbers: the future of perovskite solar cells? *Advanced Functional Materials,* 29**,** 1806482.

Li, MH, Yeh, HH, Chiang, YH, Jeng, US, Su, CJ, Shiu, HW, Hsu, YJ, Kosugi, N, Ohigashi, T & Chen, YA 2018. Highly Efficient 2D/3D Hybrid Perovskite Solar Cells via Low-Pressure Vapor-Assisted Solution Process. *Advanced Materials,* 30**,** 1801401.

Meggiolaro, D, Motti, SG, Mosconi, E, Barker, AJ, Ball, J, Perini, CaR, Deschler, F, Petrozza, A & De Angelis, F 2018. Iodine chemistry determines the defect tolerance of lead-halide perovskites. *Energy & Environmental Science,* 11**,** 702-713.

Mitzi, DB 2004. Solution-processed inorganic semiconductors. *Journal of Materials Chemistry,* 14**,** 2355-2365.

Niemegeers, A, Burgelman, M, Decock, K, Verschraegen, J & Degrave, S 2014. SCAPS manual. *University of Gent*.

Quan, LN, Yuan, M, Comin, R, Voznyy, O, Beauregard, EM, Hoogland, S, Buin, A, Kirmani, AR, Zhao, K & Amassian, A 2016. Ligand-stabilized reduced-dimensionality perovskites. *Journal of the American Chemical Society,* 138**,** 2649-2655.

Tress, W 2017. Perovskite solar cells on the way to their radiative efficiency limit–insights into a success story of high open-circuit voltage and low recombination. *Advanced Energy Materials,* 7**,** 1602358.

Zhang, F, Kim, DH & Zhu, K 2018. 3D/2D multidimensional perovskites: Balance of high performance and stability for perovskite solar cells. *Current Opinion in Electrochemistry,* 11**,** 105-113.